

"This is the peer reviewed version of the following article: "Sanz-Martín I, Permuy M, Vignoletti F, Núñez J, Muñoz F, Sanz M. A novel methodological approach using superimposed Micro-CT and STL images to analyze hard and soft tissue volume in immediate and delayed implants with different cervical designs. Clin Oral Impl Res 2018; 00:1-10", which has been published in final form at "Sanz-Martín I, Permuy M, Vignoletti F, Núñez J, Muñoz F, Sanz M. A novel methodological approach using superimposed Micro-CT and STL images to analyze hard and soft tissue volume in immediate and delayed implants with different cervical designs. Clin Oral Impl Res 2018; 29(10):986-995.

<http://doi.org/10.1111/clr.13365>"

This article may be used for non-commercial purposes in accordance with Wiley Terms and Conditions for Use of Self-Archived Versions. This article may not be enhanced, enriched or otherwise transformed into a derivative work, without express permission from Wiley or by statutory rights under applicable legislation. Copyright notices must not be removed, obscured or modified. The article must be linked to Wiley's version of record on Wiley Online Library and any embedding, framing or otherwise making available the article or pages thereof by third parties from platforms, services and websites other than Wiley Online Library must be prohibited."

A novel methodological approach using superimposed Micro- CT and STL images to analyze hard and soft tissue volume in immediate and delayed implants with different cervical designs

Ignacio Sanz-Martín¹, María Permuy², Fabio Vignoletti¹, Javier Nuñez¹, Fernando Muñoz², Mariano Sanz¹

¹Section of Periodontology, Faculty of Odontology, University Complutense of Madrid, Madrid, Spain

²Faculty of Veterinary Lugo, University of Santiago de Compostela, Lugo, Spain

Correspondence

Ignacio Sanz-Martín, Facultad de Odontología, Universidad Complutense de Madrid, Madrid, Spain.

Email: ignaciosanzmartin@odon.ucm.es

Funding information

This study was partially funded by a research grant from MIS implants technologies (Bar-Lev Industrial Park Israel). Dr. Ignacio Sanz-Martín and Dr. Mariano Sanz Alonso have received lecture fees from MIS Implants.

Abstract

Objectives: To study the hard and soft tissue volume after placing immediate (IMI) or delayed implants (DLI) with a triangular coronal macro-design (Test/T) or a conventional cylindrical design (Control/C).

Material and Methods: T/C implants were inserted in healed ridges or in fresh extraction sockets of eight beagle dogs. Biopsies were processed for Micro-CT analysis and dental stone casts were optically scanned to obtain STL files revealing the soft tissue contours at 12 weeks. Image analysis software was utilized to match common landmarks superimposing the two sets of data. Three distinct volumes were calculated; buccal bone volume (B-BV), soft tissue volume below the implant shoulder (EC-STV), and the soft tissue volume above the implant shoulder (SC-STV). Using linear measurements, the soft tissue height (STH), the mucosal thickness (MT-IS), and the distance from the implant shoulder to the bone crest (I-BC) were assessed in the digital images and in conventional histology to assess the concordance, reproducibility, and reliability.

Results: There were no significant differences between test and control implants regarding the buccal bone volume, although test implants had greater B-BV in all locations except for PM2. The

soft tissue volume was similar at T/C implants. The surgical approach influenced the distribution of the total tissue volume. In the IMI, a low position of the bone crest was correlated with low values of B-BV, SC-STV, MT-IS, and STH. Linear measurements showed a high correlation between the histology and digital measurements and high inter and intra examiner agreement.

Conclusion: The superimposition of Micro-CT/STL allowed the analysis of soft and hard tissue volumes. Reduction of the implant buccal aspect resulted in nonsignificant higher bone volume although similar soft tissue volume while the surgical approach influenced soft tissue response.

KEYWORDS

animal model, bone volume, dental implants, dimensional alterations, immediate implant, micro-CT, soft tissue volume, volumetric analysis

1 INTRODUCTION

As treatments with dental implants have become more reliable and widespread with the general population, the focus has shifted from osseointegration to the esthetic appearance of the implant restorations and the harmony with the adjacent tissues (Cairo, Sanz, Matesanz, Nieri, & Pagliaro, 2012). These aspects are heavily influenced by the widely studied physiologic changes that occur after tooth extraction, which often create soft and hard tissue deficiencies, hence, influencing the esthetic appearance of the prosthetic restorations and the peri-implant tissues.

To compensate or reduce these changes, different bone regenerative interventions have been proposed depending on the degree of crestal bone resorption (Sanz-Sanchez, Ortiz-Vigon, Sanz-Martin, Figuero, & Sanz, 2015), as well as interventions aimed to increase the mucosal thickness by means of soft tissue grafts or soft tissue substitutes (Thoma, Buranawat, Hammerle, Held, & Jung, 2014). Recent research has pointed out that the dimensional changes occurring after dental extractions not only relate to changes in bone morphology but also to those occurring at the soft tissue level (Araujo, Silva, Mendonca, & Lindhe, 2015). Chappuis and co-workers reported a 7.5-fold increase in soft tissue thickness after tooth extraction in patients with a thin bio-type hypothesizing that a rapidly resorbing thin buccal plate favoured soft tissue ingrowth and therefore increased soft tissue thickness (Chappuis et al., 2015). Moreover, experimental studies have shown an inverse correlation between peri-implant mucosal thickness and buccal bone thickness, indicating that vestibular bone deficiencies occurring at implant sites may be physiologically compensated by an increase in soft tissue thickness (Schwarz, Sager, Golubovic, Iglhaut, & Becker, 2016).

Interestingly, tissue thickness has also been shown to have an impact on the degree of bone resorption that occurs after abutment connection. In a prospective controlled clinical trial, Puisys and Linkevicius concluded that (a) when mucosal tissues are of 2 mm or less significantly more bone resorption might be expected and that (b) vertically thickened tissues seemed to behave similarly to natural thick soft tissue (Puisys & Linkevicius, 2015). These results point out to the importance of having an adequate soft and hard tissue quantity around dental implants, and hence, procedures aimed to provide enough hard and soft tissues have been routinely introduced in modern implant practices. In spite of this, the relative contribution of the soft and hard tissue to the total volume and their mutual interplay is poorly understood.

The introduction of soft tissue volumetric analysis using optical scanning and STL image superimposition has allowed the evaluation of changes in tissue contours (Benic, Wolleb, Sancho-

Puchades, & Hammerle, 2012). Using this methodology, we have gained knowledge on the impact of different treatment strategies aimed to augment tissue volume and further to assess its stability over time (Sanz Martin, Benic, Hammerle, & Thoma, 2016; Schneider, Grunder, Ender, Hammerle, & Jung, 2011). This technology, however, has certain limitations since it only provides information at the soft tissue level precluding the understanding of the soft and hard tissue inter- play. In recent years, micro-computed tomography (Micro-CT) has been extensively tested and proven as a valid method for the assessment of bone volumes (Bissinger et al., 2016; de Barros, Novaes, Carvalho, & Almeida, 2016). Thus, we have hypothesized that by merging Micro-CT technology with STL image analysis, we could obtain valid information on the relative interaction of the soft and hard tissues in the peri-implant tissue volume. It is, therefore, the purpose of this experimental in vivo investigation to analyze the relative differences in soft and hard tissue volumes, when two types of implant cervical designs (cylindrical and triangular) were placed either immediately or in healed ridges.

2 MATERIAL AND METHODS

This preclinical in vivo investigation was designed as a prospective, randomized controlled study using eight adult beagle dogs with a weight ranging between 10 and 20 kg. The experimental study was carried out at the Experimental Surgical Centre of the Hospital “Gomez-Ulla” in Madrid, Spain, once the Regional Ethical Committee for Animal Research approved the study protocol (Code: ES280790000187). This investigation reports the results from a subset analysis of the specimens whose histological results are reported in a separate publication (Sanz-Martin et al., 2017).

2.1 Implants and study design

Implant prototypes with cylindrical (control) and triangular (test) cervical design (MIS Implants Technologies Ltd., Bar-Lev Industrial Park, Israel) with a diameter of 3.5 mm and internal hexagonal connection were placed (Figure 1), either immediately after the extraction of the mesial root of third and fourth lower premolars (PM3 and PM4) with minimal flap elevation (IMI), or in the healed sites of the second pre-molars (PM2) and the mesial root of the first lower molar (M1) which had been previously extracted 8 weeks before (DLI) (Figure 2a–c). A

random assignment by computer software (SPSS Version 20.0, IBM Corporation, New York, USA) allowed that both test and control implants were evenly distributed within IMI and DLI sites as well as in the different mandibular regions.

Twelve weeks after implant placement, animals were euthanized and tissue blocks containing the implants were obtained. Each block was placed into a sealable sample container with formalin 4% solution at appropriate temperature (5°C) for storage until processing. Then, samples were dehydrated in a graded series of ethanol solutions and embedded in a light-curing resin (Technovit 7200 VLC; Heraeus-Kulzer GMBH, Werheim, Germany).

2.2 Micro-CT analysis and DICOM image acquisition

Once embedded in resin, the specimens were scanned using a high-resolution Micro-CT (Skyscan 1172, Bruker Micro-CT NV, Kontich, Belgium). The X-ray source was set at 100 Kv and 100 µA with a voxel size of 12 µm and the use of an Aluminum/ Copper filter (Al/Cu). The

scanning was performed 360° around the specimens fixed on the object stage and images were obtained every 0.4°. Once scanned, the images were re-constructed with the NRecon® software (Bruker microCT NV, Kontich, Belgium) using the algorithm described by Feldkamp (Feldkamp, Davis, & Kress, 1984). The obtained images were evaluated with the Data Viewer® software (Bruker microCT NV, Kontich, Belgium) and were re-oriented, re-sliced, and re-aligned to ensure that the implant was perfectly in alignment.

This reorientation involved recalculation of the data set where interpolation of the 2D images was done to perform the 3D analysis.

2.3 STL image acquisition

Mandibular impressions were obtained at the time of sacrifice with individualized acrylic impression trays using the one-step/two-viscosity technique with silicone impression materials (Express2 Putty Soft/Express2 Light Body, 3 M Espe, St. Paul, MN, USA). Dental stone casts were then obtained (Elite Model, Zhermack. Rome, Italy) resulting in eight models, which once evaluated for the presence of irregularities, porosities, undefined gingival margins, broken cusps, or undefined vestibulum were optically scanned with a desktop 3D scanner (Zfx Evolution Scanner, Zimmer Dental. Bolzano, Italy), thus generating STL files.

2.4 DICOM—STL image superimposition

DICOM and STL files were uploaded to an image analysis software with a specially developed purpose design plug-in (Swissmeda Software, Swissmeda AG, Zürich, Switzerland). The DICOM files obtained from the Micro-CT containing the bone and implant information were compressed and uploaded into the software in order to be matched with the soft tissue information of the STL files. Each DICOM file contained the information of one single implant while the STL files had the information of the complete mandible. The implant abutment and the adjacent teeth were the common landmarks selected as references in both sets of files to allow for an adequate matching. If the abutment was not clearly visualized the matching was not possible and the implant was excluded from the analysis. The matching was performed focusing on one single implant, for this purpose the common references in the fixed surface (Micro-CT) and the moving surface (STL) were selected via “point picking.” The point pairs generated in this manner were then transformed into pairs of point/planar CAD elements. These pairs were initially used as the input

for the “Best-fit” algorithm to compute the rigid body transformation minimizing the least square error of the distances of the points to the planar CAD elements. This process was then repeated a minimum of three times selecting additional pairs of points until the overall movement fell below a threshold of 0.01 mm (Figure 3a). A further STL image depicting the implant was used with its specific cervical design and length and matched to the implant in the Micro- CT image (Figure 3b). Care was taken that the triangle and internal hexagon fitted precisely in the cross-sectional views.

2.5 Volume computations

Once the matching was considered adequate, five curves outlining the buccal bony contours based on the information from the cross- sectional images of the Micro-CT were created. An area of interest was defined that extended 4 mm apico-coronally below the implant shoulder. This area was drawn with the intent to cover the extent of the surface reduced in the triangular cervical design. Mesio-distally, the volume analyzed extended the entire buccal width of the implant body (3.5 mm). Volume computations resulted in values in mm³.

Three distinct volumes of interest were defined; the volume enclosed between the implant surface and the outline of the buccal bone (Buccal bone volume/B-BV) which included marrow spaces, the volume enclosed between the buccal soft tissue contour below the implant shoulder and the buccal bone (Epicrestal soft tissue volume/EC-STV) and the volume enclosed between the buccal soft tissue contour above the implant shoulder and the implant abutment (Supracretal soft tissue volume/SC-STV) (Figure 4). If there was bone coronal to the implant shoulder, the software calculated the volume of bone above the implant shoulder. This value was subtracted from SC-STV and added to the B-BV.

2.6 Linear measurements

A longitudinal slice that divided the implant mesio-distally into two equal parts was selected. A line coinciding with the axis of the implant was then drawn in the transversal images of the sections.

The following linear measurements were performed by a calibrated evaluator (Figure 4);

1. I-BC: Vertical distance from the implant shoulder to the most coronal extension of the bone crest.
2. MT-IS: horizontal mucosal thickness at the implant shoulder.

3. STH: vertical soft tissue height from the implant shoulder.

2.7 Validation of the Methodology

For the purpose of assessing the concordance, reliability, and re- producibility of the presented methodology, cross-sectional images taken from the superimposition of the—CT and the STL files and were compared to the histological sections taken from the ground section process that was later performed (Figure 3b,c). Care was taken that the sections from Micro-CT/STL superimposition would represent the mesio-distal center of the implant as depicted in the histological section. To assess that the image selected in the Micro- CT/STL image corresponded with the exact same histologic cut, the two images (Micro-CT/STL and Histology) were superimposed with the aid of an image software (Adobe Photoshop Elements 15, Adobe systems. San Jose, USA) to assure that the buccal and lingual contours of the crest were identical. The implant abutment and implant outline were used as references to match the two images. Furthermore, the anatomy of the buccal bone (including marrow spaces and crestal configuration) was checked to assure that the image represented the same cross-sectional view. If the images did not match appropriately, a new cross-sectional Micro-CT/STL image was selected and the process was then repeated. Two calibrated investigators (ISM/MP) performed the measurements in the Micro- CT/STL images and in the histological sections to assess the location of the buccal and lingual I-BC, MT-IS, and STH. The values obtained from the Micro-CT and histological sections were compared as well as the values obtained from each investigator. Moreover, one investigator (ISM) performed the measurements in duplicate to assess their reproducibility.

In order to assess the accuracy of the registration further tests were performed. For this purpose, cross-sectional images that di- vided the abutment into two equal halves were selected and the diameter of the abutment was assessed in both the Micro-CT and STL files and compared against the known diameter provided by the manufacturer (diameter healing abutments = 3.5 mm).

2.8 Statistical analysis

Descriptive statistics (means, standard deviations) of the continuous variables were analyzed using a statistical software program (SPSS Version 20.0, IBM Corporation. New York, USA). The data were tested for normality by means of a Shapiro–Wilk test. A General linear model test with Bonferroni correction was used to analyze differences in the volumetric and linear measurements. To disclose associations between continuous variables, the Pearson correlation test was utilized. In order to determine the reproducibility of the linear measurements, when compared to histology

(concordance), the Passing–Bablok estimation of regression (PBR) line was determined (Passing & Bablok, 1983). In this regression line, two parameters were interpreted: (a) the constant with its 95% confidence interval (A, 95% CI), indicating constant differences between methods, when it is statistically different from 0; (b) The slope (B, 95% CI) indicating the existence of proportional differences between methods, when it is significantly different from 1. In addition, Lin's Concordance correlation coefficient (LCC) of absolute agreement (r) was calculated (Lin, 1989). The Bland– Altman interval of agreement was utilized to assess the differences between the known diameter of the implant abutment and the diameter measured in the Micro-CT and STL files. To assess inter and intra examiner agreement, the intraclass correlation coefficient (ICC) was calculated. Statistical significance was set at the alpha level of 0.05.

3 RESULTS

During the experimental investigation, the health status of the treated animals was considered as uneventful. There were no reported complications after the implant surgical procedures; all implants showed clinical evidence of integration at the time of sacrifice.

Of the initial 32 biopsies with an integration time of 12 weeks, two biopsies (1T, 1C) were excluded since matching was not possible due to the loss of the healing abutment, which prevented adequate references to perform the matching.

3.1 Volumetric assessment (primary outcome)

The image reconstructions of the volumes analyzed for the two implants (test and control) and the two sites (IMI and DLI) are shown in Figure 5. The results from the volumetric computations stratified by implant site are presented in Table 1.

There were no significant differences between test and control implants for any of the parameters analyzed. Test implants, however, had greater B-BV in all locations except in PM2 where values showed similar volumes ($15.77 \pm 7.29 \text{ mm}^3$ and $16.39 \pm 7.47 \text{ mm}^3$ for test and control, respectively). In M1, these values were of $24.71 \pm 5.44 \text{ mm}^3$ for the test implants and $21.89 \pm 4.28 \text{ mm}^3$ for the control implants. In the immediate group, at the PM3 site, the values were of $12.84 \pm 4.21 \text{ mm}^3$ in the triangular cervical design and $9.1 \pm 2.21 \text{ mm}^3$ for the cylindrical design. In the PM4, the volume of buccal bone was of $16.89 \pm 7.23 \text{ mm}^3$ for the test and $14.66 \pm 5.56 \text{ mm}^3$ for the control implants.

DLI had greater buccal bone volume overall. Within each group, the DLI at the M1 sites had greater B-BV than in PM2, while IMI implants in PM4 had greater values than those in PM3.

The total tissue volume under the implant shoulder (B-BV +EC-STV) was greater for DLI when compared to IMI; however, these values were homogeneous between PM2 and M1 (DLI) and between PM3 and PM4 (IMI). Less voluminous ridges, such as those found in PM2 and PM3, tended to have greater volume of soft tissue below the implant shoulder (EC-STV) when compared to larger ridges such as those in M1 and PM4.

Above the implant shoulder, the SC-CTV did not seem to be influenced by the implant design. However, there were noticeable differences when comparing the implant sites. M1 sites had greater soft tissue volume when compared to PM2 sites. The values in the IMI were more similar

although still favored the PM4 sites.

The distribution of the total tissue volume (TTV) shown in percentages can be found in Table 2. The percentage of the TTV occupied by the EC-STV remained rather stable in all implant sites representing about one third of the total volume. The percentage of B-BV had greater variability. Those sites that had initially lesser absolute values of B-BV (PM2 and PM3) had lower percentages (range of 19%–26%) of the TTV occupied by bone. Sites that had more voluminous ridges (M1 and PM4) had higher percentages of the TTV occupied by bone, ranging between 30% and 36%. The greatest variability was observed in the percentage of SC-STV, where M1 and PM4 sites, despite having higher absolute numbers, had a lower percentage of the TTV occupied by the soft tissue above the implant shoulder when compared to PM2 and PM3.

3.2 Linear measurements

Descriptive statistics of the linear measurements stratified by implant site are depicted in Table 1. The implant cervical design did not seem to have an influence in the parameters analyzed and the differences were not significant. The I-BC ranged from 0–40 to 0.84 mm in the delayed implants while in the immediate group this parameter ranged from 0.26 to 0.71 mm. The soft tissue height above the implant shoulder was similar for all implant sites and cervical designs and ranged from 2.5 to 3.5 mm. The horizontal mucosal thickness was also comparable with greater thickness at M1 sites and values with <0.5 mm differences between test and control implants in all sites.

3.3 Correlations between linear and volumetric data

The results of the correlation coefficients and *p*-values that relate volumetric and linear measurements can be found in Table 3. In the IMI, significant positive correlations were found between B-BV and SC-STV, B-BV and STH, B-BV, and MT-IS. High I-BC values (low position of bone crest) were correlated with low values of B-BV, SC-STV, MT-IS, and STH. In the DLI, significant positive correlations were observed between MT-IS and B-BV and SC-STV, while I-BC was positively correlated to EC-STV.

3.4 Concordance, reproducibility, and reliability of the methodology

Table S1 provides with the results of the PBR, the LCC, and the inter and intra examiner agreement providing the ICC. Overall, when the Micro-CT-STL evaluations were compared against the standard

method (histology) the concordance was high for the measurements performed. The values of A (constant differences) in the PBR analysis revealed that the I-BC measurements showed the lowest values (0.007) while the soft tissue values had superior parameters (STH = 0.14, MT = 0.317). The LCC showed values above 0.80 for all measurements. The inter and intra examiner comparisons showed generally high ICC values (>0.90 and >0.87, respectively).

The diameter of the healing abutments measured in the STL files amounted to 3.52 ± 0.03 mm with a mean difference to the value given by the manufacturer of 0.013 mm, while the diameter in the Micro-CT files was 3.53 ± 0.03 mm and a mean difference of 0.039 mm. Figure S1 depicts the Bland–Altman plot to assess the agreement of the respective Micro-CT and STL measurements of the implant abutment. Overall, as it can be appreciated, the differences between the two methods were consistently between 0.07 and -0.05 mm. When compared to the known diameter of the abutment the Micro-CT and STL tended to over-estimate the dimension of the abutment by 0.02 and 0.03 mm as can be observed by the mean diameters of the abutments for both modalities.

4 DISCUSSION

This experimental in vivo study presented a methodology to evaluate the differences in the buccal soft and hard tissue volumes when using two different implant designs at the cervical portion, which were placed either immediately in fresh extraction sockets or in healed sites. Although no significant differences were found in most of the sites, the buccal bone volume was higher for test implants in both surgical protocols. Implants with a triangular section in the cervical portion resulted in an increased distance to the socket buccal plate when placed in fresh extraction sockets and similarly, in an increased space to the buccal wall of the implant osteotomy when placed in healed ridges. This extra space, probably allowed for more bone ingrowth, what resulted in a greater bone volume attained in all sites except in PM2. In these sites, the thin buccal plate that resulted after the osteotomy preparation may have undergone extensive resorption and levelled off any possible differences between test and control implants. This modified triangular implant cervical geometry, however, did not influence the soft tissue volume above or below the implant shoulder.

Differences in soft and hard tissue healing of IMI and DLI have recently received considerable attention, although mainly through the evaluation of two-dimensional changes by means of conventional ground histology (Passoni et al., 2016; Yi et al., 2016). The methodology employed in the present investigation using both STL and Micro-CT superimposed images allowed us to evaluate three-dimensional soft and hard tissue data. Micro-CT has recently been used to evaluate peri-implant bone volume changes (Becker, Klitzsch, Stauber, & Schwarz, 2016), while STL image analysis has been validated and extensively used for the analysis of soft tissue volumetric changes around teeth and implants (Fickl et al., 2009; Schneider et al., 2011; Windisch et al., 2007). The methodology introduced based on the superimposition of the obtained DICOM and STL files allowed for volumetric comparisons and the assessment of the soft and hard tissue interplay. The analysis performed in the cross-sectional histologic and Micro-CT/STL images revealed a high concordance of the linear measurements and a high inter and intra examiner agreement. Overall, the comparison of the linear measurements obtained in the histologic and Micro-CT/STL proved to have LCC's consistently above 0.90 for the IBC and above 0.80 for STH and MT. Lower differences were also found in the PBR test when analyzing the IBC values when compared to the STH and MT. Since the STL's depicting, the soft tissues were obtained before sacrifice, these differences may be explained by the contraction that the tissues experiment after formaldehyde fixation and ethanol bathing for histological processing. The inter and intra examiner comparisons generally showed high ICC values.

The volumetric analysis performed, provided the quantification of the soft tissue volume above and below the implant shoulder, but also evaluated the effect of the implant design and the surgical protocol on the differential tissue volumes. While the modified implant cervical design had an impact on the hard tissue volume, the different surgical approaches (immediate vs. delayed) had a noticeable repercussion on both hard and soft tissues.

Moreover, the distinct characteristics of the four sites where the DLI and IMI were placed also resulted in differential outcomes. The M1 site, which corresponded to a wider crest at baseline, resulted in higher bone volumes when compared to PM2. Similarly, PM4 sites, with greater socket dimensions, resulted in higher bone volumes when compared to PM3 sites. Interestingly, in those sites with lesser buccal bone volumes, the soft tissue volume below the implant shoulder was higher. These findings are in agreement with a recently published investigation that evaluated three-dimensionally the fate of buccal soft and hard tissue eight weeks after extraction and before delayed implant placement (Chappuis et al., 2015). The authors observed a spontaneous soft tissue thickening in thin bone phenotypes 8 weeks after tooth extraction.

Similarly, DLI, in particular at M1 sites, resulted in greater soft tissue volume above the implant shoulder when compared to IMI. The impact of soft tissue volume above the implant shoulder has clear esthetic implications as it influences the contour of the alveolar ridge and the color of the peri-implant tissues (Bressan et al., 2011; Jung et al., 2008). Recently published clinical investigations have observed that DLI achieved superior esthetic results when compared to IMI (Tonetti et al., 2017). The findings of the present study suggest that IMI may need additional soft tissue grafting to enhance the soft tissue volume on the transition zone from the implant shoulder to the gingival margin to compensate the dimensional changes that occur after tooth extraction. In fact, a recently published systematic review reported that the addition of connective tissue grafting at IMI was able to increase the facial gingival thickness and ridge dimensions although it concluded that more evidence was needed to assess its potential impact on implant esthetics (Lee, Tao, & Stoupel, 2016).

When looking at the correlations in the IMI, the position of the bone crest had a clear influence on the soft tissue volume above the implant shoulder, the soft tissue height and the mucosal thickness at the implant shoulder. These findings reinforce the need of clinical strategies aimed toward minimizing the hard tissue changes that occur after IMI through the use of scaffolding materials (Sanz, Lindhe, Alcaraz, Sanz-Sanchez, & Cecchinato, 2016). On the contrary, the position of the bone crest at DLI did not seem to influence the previously mentioned soft tissue parameters. These findings highlight the impact of the surgical approach on the interplay between soft and hard tissues. It can be hypothesized that displacement of the soft tissue toward the buccal aspect in the DLI may have

masked the likely hard tissue changes. A recently published investigation that followed 22 patients over 18 months tested this particular hypothesis. All patients received DLI that showed a facial bone dehiscence <5 mm at implant placement and were randomly allocated to the augmentation group or left for spontaneous healing. Small bony dehiscence defects allocated to spontaneous healing demonstrated high implant survival rates with healthy and stable soft tissues although these sites revealed greater vertical bone loss at the buccal aspect in the first 6 months after implant insertion (Jung et al., 2016). It must be acknowledged that the present study had some limitations. The data presented were based on a low number of specimens from an experimental in vivo study, what may be insufficient to draw conclusions that can be applied in clinical practice. Furthermore, due to the lack of baseline three-dimensional hard and soft tissue data, the analysis performed was an endpoint assessment, which hindered the possibility of studying the dynamic changes of tissues over time.

Additionally, cross-sectional images were used to validate a methodology that evaluated volumetric measurements. Although histomorphometry represents a reliable method to assess anatomical landmarks, conventional volumetric calculations would have been more appropriate although would have required more invasive methods that would have hindered the histologic evaluation. Nevertheless, the methodology utilized combining the hard tissue information obtained from Micro-CT with the optical scanning of the soft tissues around implants proved to have high reliability when compared to the histological values, high reproducibility and finally high accuracy when comparing known distances to those measured in the Micro-CT and STL. This methodology may give further insights in experimental research to better understand the dynamics of tissue healing around dental implants in a three-dimensional fashion and also to discern the hard and soft tissue interplay and the reciprocal role that they may have which may provide information on their importance in the stability of the peri-implant tissues.

5 CONCLUSION

The results of the present investigation demonstrated that the superimposition of Micro-CT and optical surface scanning (STL) was effective in analyzing the volume of soft and hard tissue. Triangular implants resulted in nonsignificant higher buccal bone volumes and similar soft tissue volumes when compared to cylindrical implants.

Marked differences were observed in the soft and hard tissue volume of delayed and immediate sites.

ACKNOWLEDGEMENTS

The authors highly appreciate the contribution and work of Stephan Schmäzle and Florian Schober from Swissmeda on the image analysis software. The authors also acknowledge the help and support received from the staff at the Experimental Surgical Centre of the Hospital “Gomez-Ulla” and Dr. Javier Sanz-Esporrín and Dr. Elena Figuero for the support with the statistical analysis.

REFERENCES

Araujo, M. G., Da Silva, J. C., De Mendonca, A. F., & Lindhe, J. (2015). Ridge alterations following grafting of fresh extraction sockets in man. A randomized clinical trial. *Clinical Oral Implants Research*, 26, 407–412.

Becker, K., Klitzsch, I., Stauber, M., & Schwarz, F. (2016). Three-dimensional assessment of crestal bone levels at titanium implants with different abutment microstructures and insertion depths using micro-computed tomography. *Clinical Oral Implants Research*, 28(6), 671–676. <https://doi.org/10.1111/clr.12860>

Benic, G. I., Wolleb, K., Sancho-Puchades, M., & Hammerle, C. H. (2012). Systematic review of parameters and methods for the professional assessment of aesthetics in dental implant research. *Journal of Clinical Periodontology*, 39(Suppl 12), 160–192.

Bissinger, O., Kirschke, J. S., Probst, F. A., Stauber, M., Wolff, K. D., Haller, B., ... Kolk, A. (2016). Micro-CT vs. whole body multirow detector CT for analysing bone regeneration in an animal model. *PLoS One*, 11, e0166540.

Bressan, E., Paniz, G., Lops, D., Corazza, B., Romeo, E., & Favero, G. (2011). Influence of abutment material on the gingival color of implant-supported all-ceramic restorations: A prospective multicenter study. *Clinical Oral Implants Research*, *22*, 631–637.

Cairo, F., Sanz, I., Matesanz, P., Nieri, M., & Pagliaro, U. (2012). Quality of reporting of randomized clinical trials in implant dentistry. A systematic review on critical aspects in design, outcome assessment and clinical relevance. *Journal of Clinical Periodontology*, *39*(Suppl 12), 81–107.

Chappuis, V., Engel, O., Shahim, K., Reyes, M., Katsaros, C., & Buser, D. (2015). Soft tissue alterations in esthetic postextraction sites: a 3-dimensional analysis. *Journal of Dental Research*, *94*, 187S–193S. <https://doi.org/10.1177/0022034515592869>

De Barros, R. R., Novaes, A. B. Jr, De Carvalho, J. P., & De Almeida, A.L. (2016). The effect of a flapless alveolar ridge preservation procedure with or without a xenograft on buccal bone crest remodeling compared by histomorphometric and microcomputed tomographic analysis. *Clinical Oral Implants Research*, *28*, 938–945.

Feldkamp, L. A., Davis, L. C., & Kress, J. W. (1984). Practical cone-beam algorithm. *Journal of the Optical Society of America*, *1*, 612–619. <https://doi.org/10.1364/JOSAA.1.000612>

Fickl, S., Schneider, D., Zuhr, O., Hinze, M., Ender, A., Jung, R. E., & Hurzeler, M. B. (2009). Dimensional changes of the ridge contour after socket preservation and buccal overbuilding: An animal study. *Journal of Clinical Periodontology*, *36*, 442–448.

Jung, R. E., Herzog, M., Wolleb, K., Ramel, C. F., Thoma, D. S., & Hammerle, C. H. (2016). A randomized controlled clinical trial comparing small buccal dehiscence defects around dental implants treated with guided bone regeneration or left for spontaneous healing. *Clinical Oral Implants Research*, *28*(3), 348–354. <https://doi.org/10.1111/clr.12806>

Jung, R. E., Holderegger, C., Sailer, I., Khraisat, A., Suter, A., & Hammerle, C. H. (2008). The effect of all-ceramic and porcelain-fused-to-metal restorations on marginal peri-implant soft tissue color: A randomized controlled clinical trial. *International Journal of Periodontics and Restorative Dentistry*, *28*, 357–365.

Lee, C. T., Tao, C. Y., & Stoupel, J. (2016). The effect of subepithelial connective tissue graft placement on esthetic outcomes after immediate implant placement: systematic review. *Journal of Periodontology*, *87*, 156–167. <https://doi.org/10.1902/jop.2015.150383>

Lin, L. I. (1989). A concordance correlation coefficient to evaluate reproducibility. *Biometrics*, *45*, 255–268.

Passing, H., & Bablok, W. (1983). A new biometrical procedure for testing the equality of measurements from two different analytical methods. Application of linear regression procedures for

method comparison studies in clinical chemistry, Part I. *Journal of Clinical Chemistry and Clinical Biochemistry*, 21, 709–720. <https://doi.org/10.1515/cclm.1983.21.11.709>

Passoni, B. B., Marques De Castro, D. S., De Araujo, M. A., De Araujo, C. D., Piatelli, A., & Benfatti, C. A. (2016). Influence of immediate/ delayed implant placement and implant platform on the peri-implant bone formation. *Clinical Oral Implants Research*, 27, 1376–1383.

Puisys, A., & Linkevicius, T. (2015). The influence of mucosal tissue thickening on crestal bone stability around bone-level implants. A prospective controlled clinical trial. *Clinical Oral Implants Research*, 26, 123–129.

Sanz, M., Lindhe, J., Alcaraz, J., Sanz-Sanchez, I., & Cecchinato, D. (2016). The effect of placing a bone replacement graft in the gap at immediately placed implants: A randomized clinical trial. *Clinical Oral Implants Research*, 28(8), 902–910. <https://doi.org/10.1111/clr.12896> Sanz Martin, I., Benic, G. I., Hammerle, C. H., & Thoma, D. S. (2016). Prospective randomized controlled clinical study comparing two dental implant types. Volumetric soft tissue changes at 1 year of loading. *Clinical Oral Implants Research*, 27, 406–411.

Sanz-Martin, I., Vignoletti, F., Nunez, J., Permuy, M., Munoz, F., Sanz- Esporin, J., ... Sanz, M. (2017). Hard and soft tissue integration of immediate and delayed implants with a modified coronal macrodesign: Histological, micro-CT and volumetric soft tissue changes from a pre-clinical in vivo study. *Journal of Clinical Periodontology*, 44, 842– 853. <https://doi.org/10.1111/jcpe.12747>

Sanz-Sanchez, I., Ortiz-Vigon, A., Sanz-Martin, I., Figuero, E., & Sanz, M. (2015). Effectiveness of lateral bone augmentation on the alveolar crest dimension: a systematic review and meta-analysis. *Journal of Dental Research*, 94, 128S–142S.

Schneider, D., Grunder, U., Ender, A., Hammerle, C. H., & Jung, R. E. (2011). Volume gain and stability of peri-implant tissue following bone and soft tissue augmentation: 1-year results from a prospective cohort study. *Clinical Oral Implants Research*, 22, 28–37.

Schwarz, F., Sager, M., Golubovic, V., Iglhaut, G., & Becker, K. (2016). Horizontal mucosal thickness at implant sites as it correlates with the integrity and thickness of the buccal bone plate. *Clinical Oral Implants Research*, 27, 1305–1309.

Thoma, D. S., Buranawat, B., Hammerle, C. H., Held, U., & Jung, R. E. (2014). Efficacy of soft tissue augmentation around dental implants and in partially edentulous areas: A systematic review. *Journal of Clinical Periodontology*, 41(Suppl 15), S77–S91.

Tonetti, M. S., Cortellini, P., Graziani, F., Cairo, F., Lang, N. P., Abundo, R., ... Wetzels, A. (2017). Immediate versus delayed implant placement after anterior single tooth extraction: The timing randomized controlled clinical trial. *Journal of Clinical Periodontology*, 44, 215–224.

Windisch, S. I., Jung, R. E., Sailer, I., Studer, S. P., Ender, A., & Hammerle, C. H. (2007). A new optical method to evaluate three-dimensional volume changes of alveolar contours: A methodological in vitro study. *Clinical Oral Implants Research*, 18, 545–551.

Yi, H. Y., Park, Y. S., Pippenger, B. E., Lee, B., Miron, R. J., & Dard, M. (2016). Dimensional changes following immediate and delayed implant placement: a histomorphometric study in the canine. *International Journal of Oral and Maxillofacial Implants*, 32(3), 541–546.

LEGENDS

FIGURE 1

Schematic representation of the control (cylindrical) and test (triangular) implants.

FIGURE 2

(a) Occlusal image showing the crestal incisions at PM2 and M1 delayed sites, and the extraction of the mesial root of PM3 and PM4.

(b) Test and control implants were installed in delayed and immediate sites. Test implants in this specimen were randomized to PM2 and PM4 while control implants were at PM3 and M1.

(c) Healing abutments were secured and flaps sutured with resorbable sutures.

FIGURE 3

(a) Superimposition of Micro-CT which provides information on the hard tissue structures to the optical scan of the dental casts (blue-transparent) revealing the soft tissue anatomy. The opaque structures mesial and distal of the implant are the adjacent natural teeth.

(b) Cross-sectional images of the Micro-CT. The outline of the soft tissues can be appreciated in color blue and the matching with the implant abutment. Matching of the implant STL can also be appreciated in blue.

(c) Histological ground section of the image analyzed in b that was used for the reliability measurements

FIGURE 4

Linear and Volumetric measurements. The buccal bone volume can be appreciated in dark blue, while the epicrestal volume of soft tissue can be appreciated in magenta and the supracrestal volume of soft tissue in light blue. The outline of the soft tissues can be appreciated in orange. STH, Soft tissue height; MT-IS, mucosal thickness at the implant shoulder; I-BC, distance from the implant shoulder to the most coronal part of the bone crest

FIGURE 5

Three-dimensional reconstruction of the volumetric computations. The buccal bone volume can

be appreciated in dark blue, while the epicrestal volume of soft tissue can be appreciated in magenta and the supracrestal volume of soft tissue in light blue.

(a) Image reconstruction corresponds to an immediate test implant.

(b) Immediate control implant.

(c) Delayed control implant.

(d) Delayed test implant

FIGURE S1

Bland Altman plot to assess the agreement of the respective Micro-CT and STL measurements of the implant abutment. The central horizontal line represents the mean difference between measurements (0.01mm) while the upper and lower horizontal lines represent the 95% upper confidence interval (0.07) and lower 95% confidence interval (-0.05)

TABLES

TABLE 1:

Header: Descriptive statistics (Mean \pm SD) Of volumetric measurements in mm³ stratified by implant site.

Footer: Buccal Bone Vol, buccal bone volume; SC Soft tissue Vol, Supracrestal volume of soft tissue; EC Soft tissue vol, Epicrestal volume of soft tissue; I, implant shoulder; BC, most coronal aspect of bone crest; SHT, soft tissue height; MT-IS, mucosal thickness at the implant shoulder.

TABLE 2

Header: Distribution of total tissue volume and tissue volume below the implant shoulder shown in percentages

Footer: Buccal Bone Vol, buccal bone volume; SC Soft tissue Vol, Supracrestal volume of soft tissue; EC Soft tissue Vol, Epicrestal volume of soft tissue; I, implant shoulder; BC, most coronal aspect of bone crest; STH, soft tissue height; MT-IS, mucosal thickness at the implant shoulder.

TABLE 3:

Header: Correlation between volumetric and linear measurements in delayed (blue cells) and immediate (red cells) implants

Footer: Immediate = red cells. Delayed = blue cells. * Correlation is significant at the 0.05 level (2-tailed). ** Correlation is significant at the 0.01 level (2 tailed). Buccal Bone Vol, buccal bone volume; SC Soft tissue Vol, Supracrestal volume of soft tissue; EC Soft tissue Vol, Epicrestal volume of soft tissue; I, implant shoulder; BC, most coronal aspect of bone crest; STH, soft tissue height; MT-IS, mucosal thickness at the implant shoulder.

TABLE S1

Header: Comparative measurements of histologic samples and MCT/STL file superimpositions

S1a. Comparison histology/micro-CT. Passing-Bablok Estimation of Regression and the Lin's concordance correlation coefficient.

S1b. Inter-examiner comparisons. Intra-class correlation coefficients.

S1c. Intra-examiner comparisons. Intra-class correlation coefficients.

Footer:

PBR-A, Passing-Bablok Estimation of regression constant; PBR-B, Passing-Bablok Estimation of regression slope; LCC, Lin's concordance correlation coefficient.

I, implant shoulder; BC, most coronal aspect of bone crest; STH, soft tissue height; MT-IS, mucosa thickness at the implant shoulder; MCT, Micro-CT; buc, buccal; lin, lingual.

Table 1

	Delayed						Immediate					
	PM2			M1			PM3			PM4		
	Test (n=3)	Control (n= 4)	p value	Test (n=3)	Control (n= 4)	p value	Test (n=3)	Control (n= 4)	p value	Test (n=3)	Control (n= 4)	p value
Volumetric measurements												
Buccal Bone Vol	15.77 ± 7.29	16.39 ± 7.47	0.552	24.71 ± 5.44	21.89 ± 4.28	0.522	12.84 ± 4.21	9.1 ± 2.21	0.360	16.89 ± 7.23	14.66 ± 5.56	0.584
SC Soft tissue vol	20.47 ± 1.03	16.69 ± 8.00	0.461	22.73 ± 7.96	26.75 ± 4.98	0.433	15.58 ± 6.37	17.06 ± 5.74	0.766	18.91 ± 8.96	17.51 ± 5.69	0.759
EC Soft tissue vol	24.41 ± 9.05	26.74 ± 4.2	0.242	20.21 ± 3.64	20.22 ± 8.52	0.918	20.14 ± 2.49	22.74 ± 6.92	0.537	18.06 ± 5.96	15.11 ± 4.13	0.483
Linear measurements												
I-BC	0.73 ± 0.77	0.84 ± 0.34	0.724	0.50 ± 0.10	0.40 ± 0.48	0.289	0.71 ± 0.85	0.53 ± 0.37	0.767	0.26 ± 0.30	0.32 ± 0.15	0.56
STH	2.47 ± 0.183	3.03 ± 0.68	0.157	3.42 ± 1.02	2.82 ± 0.2	0.48	2.58 ± 0.71	2.56 ± 0.33	0.564	2.81 ± 0.24	2.79 ± 0.41	0.773
MT-IS	2.51 ± 0.21	2.09 ± 1.70	0.289	2.90 ± 0.16	2.93 ± 0.36	0.957	1.80 ± 0.46	2.16 ± 0.43	0.284	2.59 ± 0.55	1.94 ± 0.43	0.183

Table 2

	Delayed				Immediate			
	PM2		M1		PM3		PM4	
	Test (n= 3)	Control (n = 4)	Test (n= 3)	Control (n = 4)	Test (n= 4)	Control (n = 4)	Test (n= 4)	Control (n = 4)
Distribution of the total tissue volume								
Buccal Bone Vol	24.61	26.32	36.78	32.23	26.24	19.18	32.1	30.66
SC Soft tissue Vol	39.23	46.97	29.91	28.94	42.75	46.36	33.92	32.36
EC Soft tissue Vol	36.14	26.69	33.3	38.81	30.99	34.44	33.97	36.97
Distribution of the tissue volume below the implant shoulder.								
Buccal Bone Vol	38.77	35.63	54.86	53.37	38.44	29.73	48.11	48.36
EC Soft tissue Vol	61.22	64.36	45.13	46.62	61.55	70.26	51.88	51.63

Table 3

		Buccal Bone Vol	SC Soft tissue Vol	EC Soft tissue Vol	I-BC	STH	MT-IS
Buccal Bone Vol	Pearson Corr.	1	0.318	-0.348	-0.304	0.029	0.592*
	<i>p</i> value		0.268	0.222	0.290	0.922	0.026
SC Soft tissue Vol	Pearson Corr.	0.601*	1	-0.295	-0.328	0.499	0.651*
	<i>p</i> value	0.014		0.306	0.252	0.069	0.012
EC Soft tissue Vol	Pearson Corr.	-0.200	0.360	1	0.658*	-0.036	-0.114
	<i>p</i> value	0.457	0.171		0.011	0.902	0.698
I-BC	Pearson Corr.	-0.581*	-0.546*	0.227	1	-0.044	-0.180
	<i>p</i> value	0.018	0.029	0.397		0.883	0.539
STH	Pearson Corr.	0.549*	0.511*	-0.008	-0.746**	1	0.112
	<i>p</i> value	0.028	0.043	0.977	0.001		0.703
MT-IS	Pearson Corr.	0.637**	0.772**	0.175	-0.636**	0.562*	1
	<i>p</i> value	0.008	0.000	0.518	0.008	0.023	

Table S1

Table S1. Comparative measurements of histologic samples and MicroCT/STL file superimpositions.				
S1a. Comparison Histology/Micro CT. Passing-Bablok Estimation of Regression and the Lin's concordance correlation coefficient.				
<i>Parameters</i>	<i>PBR-A (A, 95% CI)</i>	<i>PBR-B (B, 95% CI)</i>	<i>LCC</i>	
IBC	0.007 (-0.05-0.04)	1.01(0.89-1.11)	0.948	
STH	0.14(-0.84-0.79)	0.87(0.66-1.21)	0.802	
MT	0.317(-0.581-0.36)	1.03(0.89-1.42)	0.831	
S1b. Inter-examiner comparisons. Intraclass correlation coefficients.				
<i>Parameters</i>	<i>Histology (buc)</i>	<i>MCT/STL (buc)</i>	<i>Histology (lin)</i>	<i>MCT/STL (lin)</i>
IBC	0.99	0.975	0.997	0.991
STH	0.921	0.97	0.988	0.99
MT	0.996	0.986	0.998	0.972
S1c. Intra-examiner comparisons. Intraclass correlation coefficients.				
<i>Parameters</i>	<i>Histology (buc)</i>	<i>MCT/STL (buc)</i>	<i>Histology (lin)</i>	<i>MCT/STL (lin)</i>
IBC	0.997	0.97	0.989	0.994
STH	0.947	0.889	0.992	0.874
MT	0.973	0.978	0.981	0.989
PBR-A,Passing-Bablok Estimation of Regression constant; PBR-B,Passing-Bablok Estimation of Regression Slope; LCC, Lin's concordance correlation coefficient; I, implant shoulder; BC,most coronal aspect of bone crest; STH, soft tissue height; MT-IS, mucosal thickness at the implant shoulder; MCT, Micro-CT; buc,buccal; lin,lingual.				



Figure 1

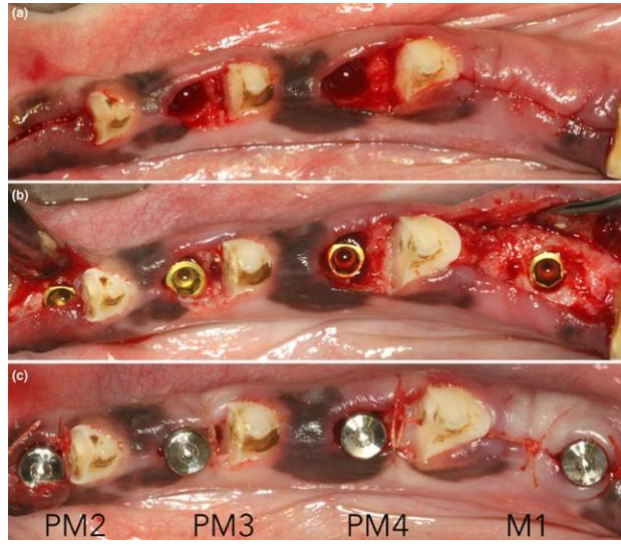


Figure 2

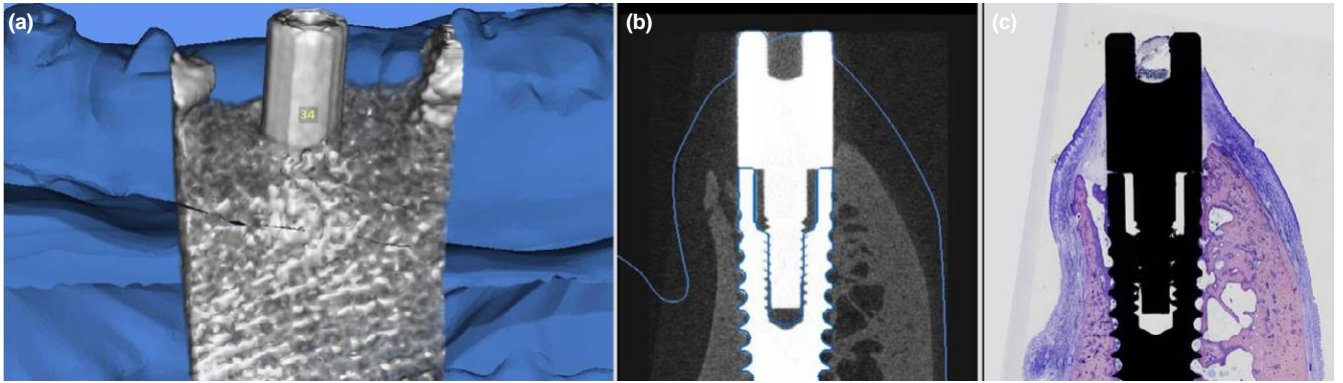


Figure 3



Figure 4

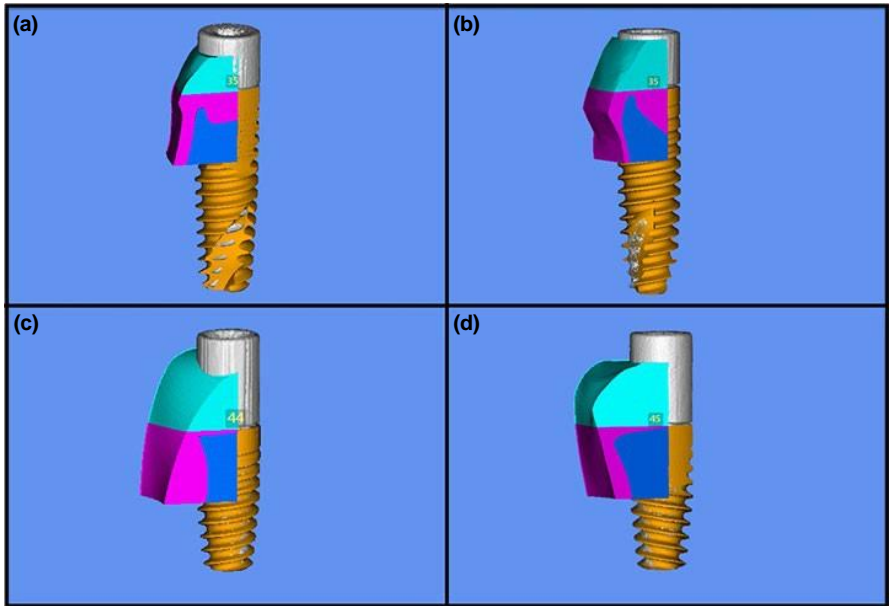


Figure 5

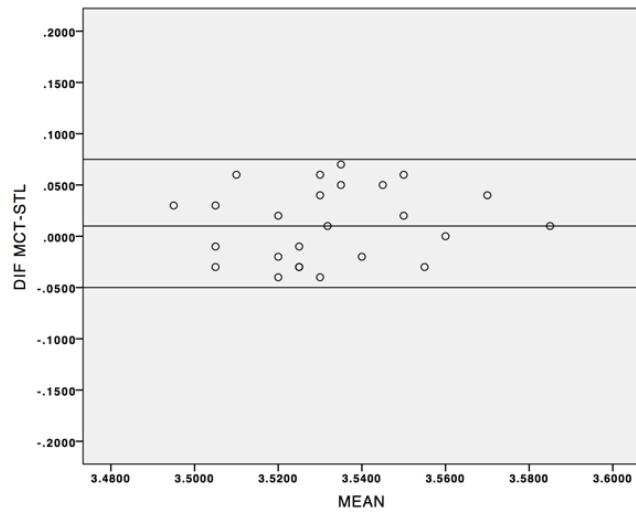


Figure S1

The ARRIVE Guidelines Checklist

Animal Research: Reporting In Vivo Experiments

Carol Kilkenny¹, William J Browne², Innes C Cuthill³, Michael Emerson⁴ and Douglas G Altman⁵

¹The National Centre for the Replacement, Refinement and Reduction of Animals in Research, London, UK, ²School of Veterinary Science, University of Bristol, Bristol, UK, ³School of Biological Sciences, University of Bristol, Bristol, UK, ⁴National Heart and Lung Institute, Imperial College London, UK, ⁵Centre for Statistics in Medicine, University of Oxford, Oxford, UK.

	ITEM	RECOMMENDATION	Section/ Paragraph
Title	1	Provide as accurate and concise a description of the content of the article as possible.	
Abstract	2	Provide an accurate summary of the background, research objectives, including details of the species or strain of animal used, key methods, principal findings and conclusions of the study.	
INTRODUCTION			
Background	3	<p>a. Include sufficient scientific background (including relevant references to previous work) to understand the motivation and context for the study, and explain the experimental approach and rationale.</p> <p>b. Explain how and why the animal species and model being used can address the scientific objectives and, where appropriate, the study's relevance to human biology.</p>	
Objectives	4	Clearly describe the primary and any secondary objectives of the study, or specific hypotheses being tested.	
METHODS			
Ethical statement	5	Indicate the nature of the ethical review permissions, relevant licences (e.g. Animal [Scientific Procedures] Act 1986), and national or institutional guidelines for the care and use of animals, that cover the research.	
Study design	6	<p>For each experiment, give brief details of the study design including:</p> <p>a. The number of experimental and control groups.</p> <p>b. Any steps taken to minimise the effects of subjective bias when allocating animals to treatment (e.g. randomisation procedure) and when assessing results (e.g. if done, describe who was blinded and when).</p> <p>c. The experimental unit (e.g. a single animal, group or cage of animals).</p> <p>A time-line diagram or flow chart can be useful to illustrate how complex study designs were carried out.</p>	
Experimental procedures	7	<p>For each experiment and each experimental group, including controls, provide precise details of all procedures carried out. For example:</p> <p>a. How (e.g. drug formulation and dose, site and route of administration, anaesthesia and analgesia used [including monitoring], surgical procedure, method of euthanasia). Provide details of any specialist equipment used, including supplier(s).</p> <p>b. When (e.g. time of day).</p> <p>c. Where (e.g. home cage, laboratory, water maze).</p> <p>d. Why (e.g. rationale for choice of specific anaesthetic, route of administration, drug dose used).</p>	
Experimental animals	8	<p>a. Provide details of the animals used, including species, strain, sex, developmental stage (e.g. mean or median age plus age range) and weight (e.g. mean or median weight plus weight range).</p> <p>b. Provide further relevant information such as the source of animals, international strain nomenclature, genetic modification status (e.g. knock-out or transgenic), genotype, health/immune status, drug or test naïve, previous procedures, etc.</p>	

Housing and husbandry	9	Provide details of: a. Housing (type of facility e.g. specific pathogen free [SPF]; type of cage or housing; bedding material; number of cage companions; tank shape and material etc. for fish). b. Husbandry conditions (e.g. breeding programme, light/dark cycle, temperature, quality of water etc for fish, type of food, access to food and water, environmental enrichment). c. Welfare-related assessments and interventions that were carried out prior to, during, or after the experiment.
Sample size	10	a. Specify the total number of animals used in each experiment, and the number of animals in each experimental group. b. Explain how the number of animals was arrived at. Provide details of any sample size calculation used. c. Indicate the number of independent replications of each experiment, if relevant.
Allocating animals to experimental groups	11	a. Give full details of how animals were allocated to experimental groups, including randomisation or matching if done. b. Describe the order in which the animals in the different experimental groups were treated and assessed.
Experimental outcomes	12	Clearly define the primary and secondary experimental outcomes assessed (e.g. cell death, molecular markers, behavioural changes).
Statistical methods	13	a. Provide details of the statistical methods used for each analysis. b. Specify the unit of analysis for each dataset (e.g. single animal, group of animals, single neuron). c. Describe any methods used to assess whether the data met the assumptions of the statistical approach.
RESULTS		
Baseline data	14	For each experimental group, report relevant characteristics and health status of animals (e.g. weight, microbiological status, and drug or test naïve) prior to treatment or testing. (This information can often be tabulated).
Numbers analysed	15	a. Report the number of animals in each group included in each analysis. Report absolute numbers (e.g. 10/20, not 50% ²). b. If any animals or data were not included in the analysis, explain why.
Outcomes and estimation	16	Report the results for each analysis carried out, with a measure of precision (e.g. standard error or confidence interval).
Adverse events	17	a. Give details of all important adverse events in each experimental group. b. Describe any modifications to the experimental protocols made to reduce adverse events.
DISCUSSION		
Interpretation/scientific implications	18	a. Interpret the results, taking into account the study objectives and hypotheses, current theory and other relevant studies in the literature. b. Comment on the study limitations including any potential sources of bias, any limitations of the animal model, and the imprecision associated with the results ² . c. Describe any implications of your experimental methods or findings for the replacement, refinement or reduction (the 3Rs) of the use of animals in research.
Generalisability/translation	19	Comment on whether, and how, the findings of this study are likely to translate to other species or systems, including any relevance to human biology.
Funding	20	List all funding sources (including grant number) and the role of the funder(s) in the study.

References:

1. Kilkeny C, Browne WJ, Cuthill IC, Emerson M, Altman DG (2010) Improving Bioscience Research Reporting: The ARRIVE Guidelines for Reporting Animal Research. *PLoS Biol* 8(6): e1000412. doi:10.1371/journal.pbio.1000412
2. Schulz KF, Altman DG, Moher D, the CONSORT Group (2010) CONSORT 2010 Statement: updated guidelines for reporting parallel group randomised trials. *BMJ* 340:c332.